The EMBO Journal vol.13 no.14 pp.3261 – 3271, 1994

The ABC-transporter Ste6 accumulates in the plasma membrane in a ubiquitinated form in endocytosis mutants

Ralf Kölling[1] and Cornelis P.Hollenberg

Institut für Mikrobiologie, Heinrich-Heine-Universität Düsseldorf, D-40225 Düsseldorf, Germany
[1]Corresponding author

Communicated by W.Neupert

We are investigating the transport and turnover of the multispanning membrane protein Ste6. The Ste6 protein is a member of the ABC-transporter family and is required for the secretion of the yeast mating pheromone a-factor. In contrast to the prevailing view that Ste6 is a plasma membrane protein, we found that Ste6 is mainly associated with internal membranes and not with the cell surface. Fractionation and immunofluorescence data are compatible with a Golgi localization of Ste6. Despite its mostly intracellular localization, the Ste6 protein is in contact with the cell surface, as demonstrated by the finding that Ste6 accumulates in the plasma membrane in endocytosis mutants. The Ste6 protein which accumulates in the plasma membrane in endocytosis mutants is ubiquitinated. Ste6 is thus the second protein in yeast besides MATα2 for which ubiquitination has been demonstrated. Ste6 is a very unstable protein (half-life 13 min) which is stabilized ~3-fold in a *ubc4 ubc5* mutant, implicating the ubiquitin system in the degradation of Ste6. The strongest stabilizing effect on Ste6 is, however, observed in the vacuolar *pep4* mutant (half-life >2 h), suggesting that most of Ste6 is degraded in the vacuole. Secretory functions are required for efficient degradation of Ste6, indicating that Ste6 enters the secretory pathway and is transported to the vacuole by vesicular carriers.

Key words: **a**-factor/mating/proteolysis/secretion

Introduction

The secretion of the yeast mating pheromone **a**-factor, a farnesylated dodecapeptide, is dependent on the Ste6 protein (Kuchler *et al.*, 1989; McGrath and Varshavsky, 1989). Ste6 is a member of the ABC-transporter family and shares substantial sequence homology with mammalian transporters like MDR and CFTR (Higgins, 1992). The predicted secondary structure and the membrane topology of these transporters are very similar. The proteins contain one or two copies of a basic repeat consisting of six transmembrane-spanning segments and a cytoplasmic domain with a putative ATP-binding fold. Ste6 and mammalian MDR proteins seem to be closely related, indicated by the ability of mouse mdr3 to complement a Ste6 defect (Raymond *et al.*, 1992). We are using Ste6 as a model protein to study the intracellular transport and turnover of membrane proteins. Knowledge of the signals and mechanisms involved in the transport of Ste6 may also contribute to the understanding of the most common defect in CFTR causing cystic fibrosis. This mutation, a deletion of phenylalanine 508, leads to a temperature-dependent mislocalization of the CFTR protein (Denning *et al.*, 1992).

In this paper, we show that Ste6 is transported to the cell surface, followed by rapid endocytosis. The existence of an endocytic pathway in yeast is now well established. Initial work focused on the Ste2 receptor-mediated uptake of the yeast mating pheromone α-factor (Riezman, 1993). The receptor-bound α-factor accumulates within the cell in an intermediate, probably endosomal compartment before it is finally degraded in the vacuole (Singer and Riezman, 1990), the organelle analogous to the lysosome. By an independent set of experiments, an intermediate compartment for the transport of the vacuolar protease CPY from the Golgi to the vacuole has been identified as another candidate for a yeast endosomal compartment (Vida *et al.*, 1993). Whether the compartments identified by these two different approaches are identical remains to be shown. Recently, the **a**-factor receptor Ste3 was established as another endocytic marker in yeast (Davis *et al.*, 1993).

Internalization and subsequent delivery to the lysosome seems to be the main route for the degradation of plasma membrane proteins (Hare, 1990). Little is known, however, about the regulation of the protein turnover and about the contribution of other pathways to the degradation of membrane proteins. Here we present evidence that Ste6 is ubiquitinated and that this ubiquitination contributes to the degradation of the Ste6 protein. One of the functions of ubiquitin is to mark proteins for degradation by the 26S proteasome. There is now extensive knowledge about the machinery required for the ubiquitination of proteins (reviewed in Finley and Chau, 1991; Hershko and Ciechanover, 1992; Jentsch, 1992). There are, however, only a few specific cellular proteins known to date where the ubiquitin system has been implicated in their degradation. The known examples are the phytochrome photoreceptor of plants (Jabben *et al.*, 1989), cyclins (Glotzer *et al.*, 1991), nuclear oncoproteins (Hershko and Ciechanover, 1992) and the yeast transcription factor MATα2 (Hochstrasser *et al.*, 1991). Several cell surface proteins, including the MEL-14 lymphocyte homing receptor (Siegelman *et al.*, 1986), the PDGF receptor (Yarden *et al.*, 1986), growth hormone receptor (Leung *et al.*, 1987), T-cell receptor (Cenciarelli *et al.*, 1992) and immunoglobulin E receptor (Paolini and Kinet, 1993) are also modified by ubiquitination. However, there is no clear correlation between the ubiquitination and the degradation of these proteins. Results obtained for the immunoglobulin E receptor rather point to a role of ubiquitination in signal transduction (Paolini and Kinet, 1993). Thus, the Ste6

protein would be the first example where there is a connection between the ubiquitination of a membrane protein and its degradation.

Results

Ste6 is associated with internal membranes

To determine the subcellular localization of the Ste6 protein we raised antibodies against a trpE–Ste6 fusion protein. The antibodies recognized a yeast protein of ~140 kDa, in agreement with the expected size of Ste6 (mol. wt = 144 744). This protein could only be immunoprecipitated from *MAT***a** and not from *MAT*α cell extracts, it was not detectable in extracts from a *MAT***a** Δ*ste6* disruption strain and it was overproduced in a *MAT***a** strain carrying the *STE6* gene on a multicopy plasmid (not shown).

The subcellular localization of Ste6 was analysed by density gradient centrifugation. Cell extracts were prepared from the *MAT***a** wild-type strain DBY2063 and loaded onto a sucrose gradient. The fractions collected from the sucrose gradient were assayed for the presence of Ste6 protein, plasma membrane ATPase (PMATPase) and the Golgi protein dipeptidyl aminopeptidase A (DPAP A) by SDS–PAGE and Western blotting. As can be seen from Figure 1A and B, the Ste6 protein and PMATPase clearly do not co-localize. The PMATPase antibodies recognize a protein of apparent mol. wt 110 kDa, the size predicted for the protein. The PMATPase equilibrates at sucrose concentrations of 45–50% (d = 1.20–1.23, where d represents density), while the Ste6 protein is found at sucrose concentrations of 27–35% (d = 1.11–1.15). Only a minor portion of Ste6 can be seen in the plasma membrane fraction. Ste6 is, therefore, predominantly associated with internal membranes and not with the plasma membrane. The distributions of Ste6 and the 112 kDa DPAP A protein (Roberts *et al.*, 1992), however, were very similar (Figure 1B and C). In fact, the distribution patterns were almost superimposable, as can be seen from Figure 1D where the signal intensities of Ste6 and DPAP A, quantitated by densitometry, are plotted against the fraction number.

To determine the position of membranes derived from other cellular compartments, marker enzymes were assayed (Figure 1D and E). The highest activity for NADPH cytochrome *c* oxidoreductase, an enzyme frequently used as an endoplasmic reticulum (ER) marker, is found at sucrose concenrations of 20–25% (d = 1.08–1.10), while α-mannosidase activity, a vacuolar marker enzyme, was detected at 25–30% sucrose (d = 1.10–1.13). It appears as if the Ste6 and DPAP A patterns seen on the sucrose gradient are generated by three overlapping peaks. One of these potential peaks seems to coincide with the major α-mannosidase peak. This is an indication that a fraction of Ste6 and DPAP A could be contained in the vacuole.

Indirect immunofluorescence experiments confirm the results obtained by cell fractionation. For these experiments, we used an epitope-tagged version of Ste6 expressed from a multicopy plasmid (Kuchler *et al.*, 1993) since the anti-epitope antibodies gave a clearer signal than the affinity-purified anti-Ste6 antibodies. In the *STE6* disruption strain JPY201 transformed with the *STE6-c-*

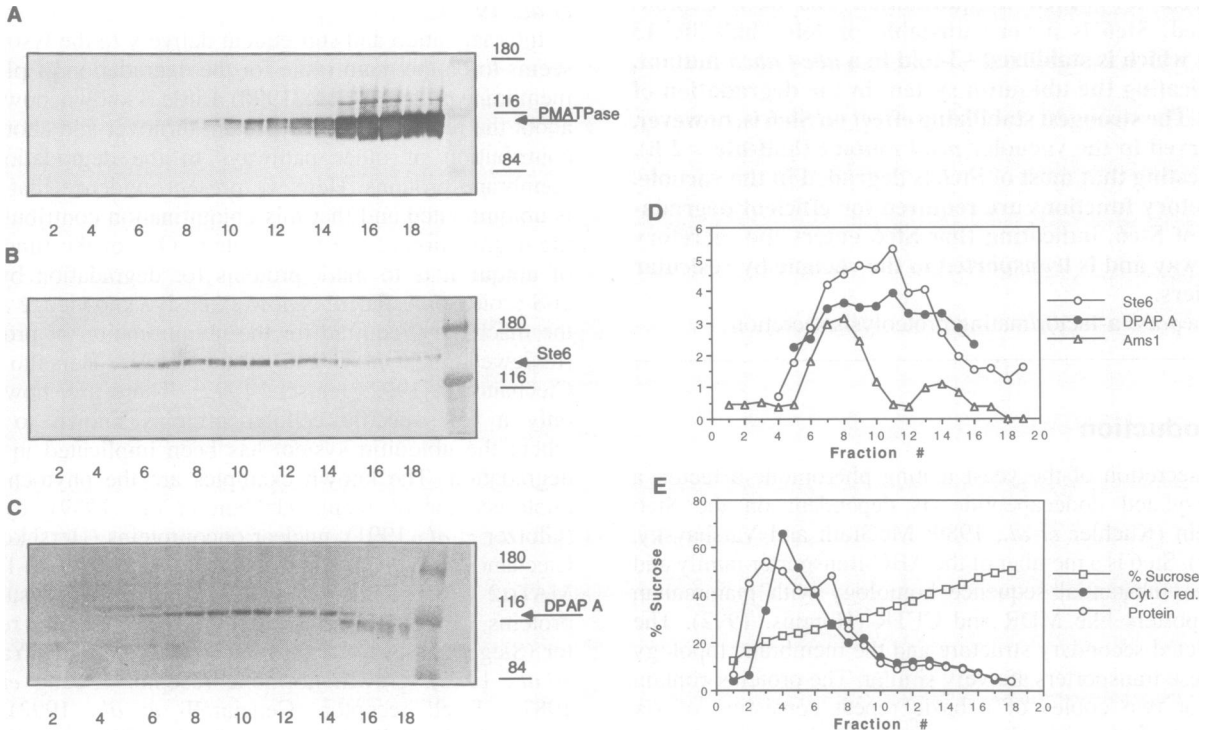

Fig. 1. Fractionation of Ste6 on sucrose gradients. A whole-cell extract of DBY2063 was fractionated by density-gradient centrifugation. Aliquots of the gradient fractions were separated on 7.5% SDS–PAGE gels and analysed by Western blotting with (**A**) anti-PMATPase antibodies, (**B**) affinity-purified anti-Ste6 antibodies and (**C**) anti-DPAP A antibodies. The sizes of marker proteins in kDa and the fraction numbers are indicated. (**D**) The α-mannosidase activity (in arbitrary units) and the intensities of the DPAP A and Ste6 Western blot signals (quantitated by densitometry) are plotted against the fraction number. (**E**) Density (% sucrose, w/w), protein concentration and NADPH cytochrome *c* oxidoreductase activity (arbitrary units) plotted against the fraction number.

myc plasmid, a dot-like staining pattern was observed with the anti-c-myc antibodies (Figure 2G and H). No surface staining was obvious. A similar staining was observed for Golgi proteins like e.g. Kex2 (Redding *et al.*, 1991). Thus, both the fractionation and the immunofluorescence experiments are compatible with a Golgi localization of Ste6. Although the staining was less bright, a similar result was obtained with the anti-Ste6 antibodies (not shown). Recently, Kuchler *et al.* (1993) described a similar patchy Ste6 staining pattern in immunofluorescence experiments with the same *STE6* plasmid. Their conclusion, however, was that Ste6 is predominantly plasma membrane associated. We think that the dot-like staining pattern is more compatible with an intracellular localization of Ste6. The addition of the c-myc epitope and the overproduction do not seem to alter the intracellular distribution of Ste6. On sucrose gradients, the fractionation behaviour of the tagged Ste6 version expressed from the multicopy plasmid was indistinguishable from single-copy, wild-type Ste6 (not shown).

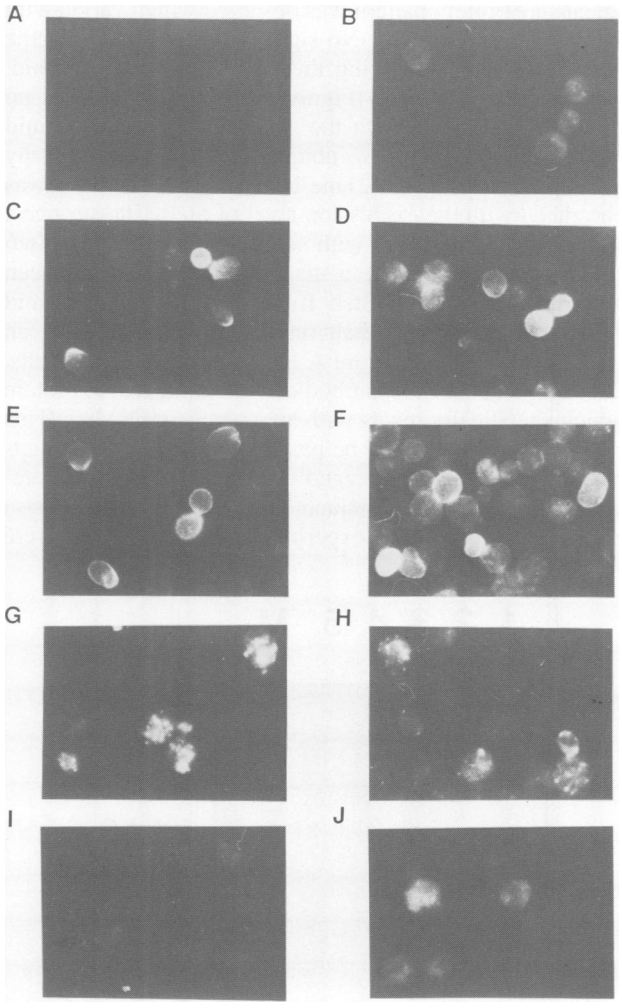

Fig. 2. Localization of Ste6 by immunofluorescence microscopy. The c-myc-tagged Ste6 protein was visualized with anti-c-myc primary antibodies and FITC-conjugated anti-mouse secondary antibodies. (A, C, E, G and I): cells grown at 25°C; (B, D, F, H and J): cells shifted to 36°C for 1 h before fixation. Strains: (**A** and **B**) RKY562 *end4 Δste6*; (**C** and **D**) RH266-1D *end3* transformed with 2μ-*STE6-c-myc* plasmid; (**E** and **F**) RH268-1C *end4* transformed with 2μ-*STE6-c-myc* plasmid; (**G** and **H**) JPY201 *Δste6* transformed with 2μ-*STE6-c-myc* plasmid; (**I** and **J**) RH266-1D *end3* transformed with 2μ-*STE6* plasmid.

Ste6 accumulates at the cell surface in endocytosis mutants

Considering the proposed role of Ste6 as an **a**-factor transporter functioning at the plasma membrane, the intracellular localization of the protein was surprising. Our results can be interpreted in two ways. First, it is possible that Ste6 is indeed an intracellular protein which would have important implications for the mechanism of **a**-factor secretion or secondly that the Ste6 protein is transported to the cell surface, but stays there only for a short period of time due to rapid internalization by endocytosis. To distinguish between these alternatives, we analysed the distribution of Ste6 in endocytosis mutants by cell fractionation and by immunofluorescence experiments. The results obtained with the *end4* mutant RH268-1C (Raths *et al.*, 1993), which has a conditional defect in the uptake of Ste2-bound α-factor, are shown in Figure 3. Cell extracts were prepared from *end4* cells grown at permissive temperature (25°C) and from cells shifted for 1 h to non-permissive temperature (36°C). Total cell extracts were fractionated on sucrose gradients. As can be

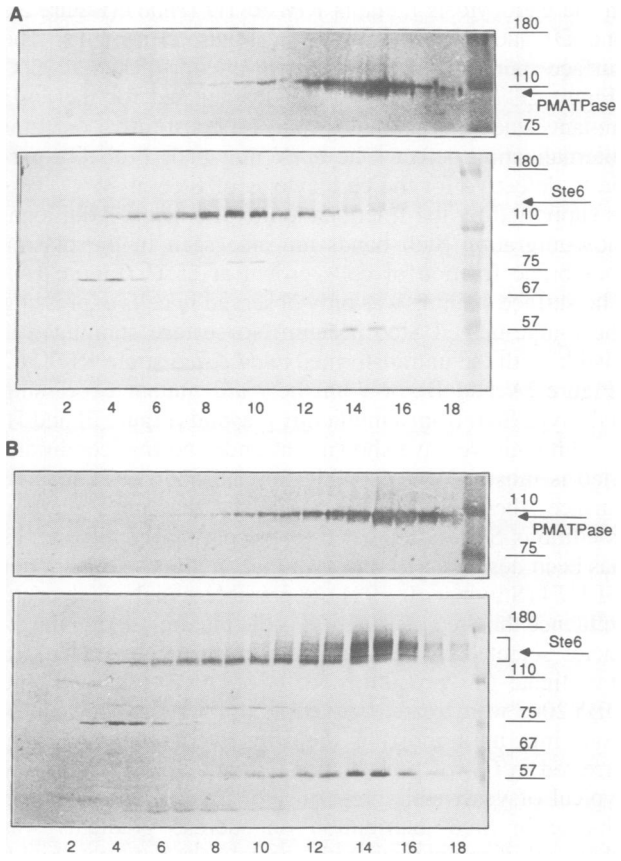

Fig. 3. Distribution of Ste6 in the endocytosis mutant *end4*. Cell extracts of the *end4* strain RH268-1C were fractionated on sucrose gradients. (**A**) Extracts from cells grown at 25°C and (**B**) from cells shifted to 36°C for 1 h prior to extract preparation. Upper panels: Western blot of gradient fractions with anti-PMATPase antibodies; lower panels: Western blot with anti-Ste6 antibodies. The sizes of marker proteins in kDa and the positions of PMATPase and Ste6 are indicated.

seen from Figure 3A, an essentially wild-type distribution comparable with that shown in Figure 1 is observed for the cells grown at permissive temperature. However, when the cells are shifted to 36°C, an accumulation of Ste6 protein in the plasma membrane fraction can be seen (Figure 3B). The mobility of the Ste6 protein in this fraction is altered, indicating that the protein is post-translationally modified. This newly accumulating material is not observed in the *end4* mutant RKY562 carrying a *STE6* deletion, confirming that what we see is indeed Ste6 (not shown).

Mutations in the yeast clathrin heavy chain, which cause a partial defect in the endocytosis of α-factor, lead to a missorting of Golgi proteins to the plasma membrane (Seeger and Payne, 1992). We therefore examined whether the Golgi proteins Kex2 and DPAP A are also found in the plasma membrane fraction in the *end4* mutant at non-permissive temperature. However, in contrast to Ste6, the Kex2 and DPAP A proteins were not detectable in the plasma membrane fraction (not shown).

We then examined the Ste6 distribution by immunofluorescence microscopy in endocytosis mutants transformed with the *STE6-c-myc* plasmid. Instead of the dot-like staining pattern seen in the wild-type strain JPY201 (Figure 2G and H), a distinct surface staining was observed in the endocytosis mutants RH266-1D (*end3*) (Figure 2C and D) and RH268-1C (*end4*) (Figure 2E and F). The surface staining was also apparent in cells grown at 25°C (Figure 2C and E). This is not unexpected for the *end3* mutant, since this mutant displays a constitutive α-factor internalization defect. The *end4* mutant is probably partially defective for the endocytosis of Ste6 at 25°C. This is supported by the fractionation experiments. Additional slow-migrating Ste6 bands are also seen in the plasma membrane fraction of cells grown at 25°C (Figure 3A). The surface staining was only observed in cells expressing the c-myc-tagged Ste6 protein. No surface staining was visible with the untransformed *end4 Δste6* strain RKY562 (Figure 2A and B) or with the *end3* mutant expressing wild-type Ste6 from a multicopy plasmid (Figure 2I and J).

Although we have shown that under normal conditions Ste6 is mostly located within the cell and not at the cell surface, there is still the possibility that under certain conditions Ste6 is relocated to the plasma membrane, as has been described for the mammalian glucose transporter GLUT4 (Smith *et al.*, 1991). A possible signal which could influence the Ste6 distribution is the mating pheromone α-factor secreted by cells of the opposite mating type. To investigate this possibility, cells of the *MAT***a** wild-type DBY2063 were treated with α-factor for about one generation time until most of the cells were unbudded (i.e. arrested in G_1) or pear shaped ('shmoos'), a morphology typical of yeast cells preparing for mating. However, no change in Ste6 distribution on sucrose gradients was observed in comparison with control cells not treated with α-factor (not shown). Therefore, it seems that under the conditions tested α-factor does not lead to a relocalization of Ste6 to the plasma membrane.

The Ste6 protein is ubiquitinated

In endocytosis mutants, a low-mobility form of Ste6 accumulates in the plasma membrane fraction at non-permissive temperature (Figure 3B). We tested whether this altered mobility was due to a ubiquitination of the Ste6 protein. Initial attempts to visualize the ubiquitination of Ste6 with anti-ubiquitin antibodies gave only weak signals. To enhance the signal, we made use of an epitope-tagged variant of ubiquitin described by Hochstrasser *et al.* (1991). The *end4 Δste6* strain RKY592 was transformed with two plasmids: one expressing ubiquitin either with c-myc tag (YEp105) or without tag (YEp96) and another expressing Ste6. Different *STE6* plasmids were used: pRK109, a single-copy *STE6* plasmid; pRK69, a multicopy *STE6* plasmid; and pRK89, a multicopy plasmid expressing the C-terminal half of Ste6.

The *CUP1* promoter-dependent expression of plasmid-encoded ubiquitin was induced by growth in Cu^{2+}-containing medium. The cells were then shifted to non-permissive temperature (36°C) for 1 h. Cell extracts were prepared and an immunoprecipitation was performed with anti-Ste6 antibodies. The precipitated proteins were analysed by Western blotting with anti-c-myc antibodies. A smear-like protein pattern was observed which varied with the *STE6* plasmid used. No signal was obtained with the *end4 Δste6* strain carrying the ubiquitin c-myc plasmid, but no *STE6* plasmid (Figure 4, lane 2). Likewise, no signal was obtained with the strain carrying the plasmid expressing the 'tag-less' ubiquitin and the single-copy *STE6* plasmid (Figure 4, lane 1). The signal intensity was correlated with the expression level of Ste6. The strongest signal was observed with cells overproducing Ste6 (Figure 4, lane 3), while a much fainter signal was seen with cells expressing Ste6 from a single-copy plasmid (Figure 4, lane 5). The half-sized Ste6 (pRK89) gave an intermediate signal (Figure 4, lane 4). From these results, it is clear that the Ste6 antibodies precipitate a Ste6 protein which specifically reacts with anti-c-myc antibodies. This protein species can only be precipitated from cell extracts containing the epitope-tagged variant of ubiquitin. Therefore, Ste6 must be conjugated to ubiquitin. We also performed the reverse experiment where proteins were

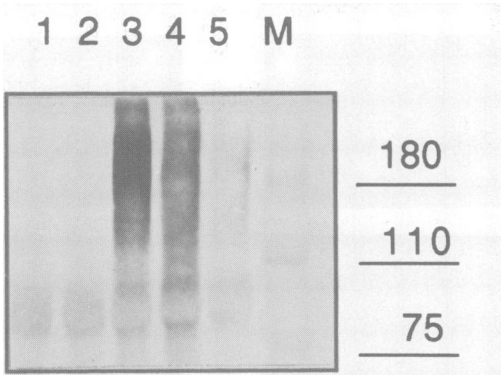

Fig. 4. Ubiquitination of Ste6. The Ste6 protein was immunoprecipitated from cell extracts with anti-Ste6 antibodies. The precipitated proteins were analysed by Western blotting with anti-c-myc antibodies. The cell extracts were prepared from the strain RKY592 *end4 Δste6* transformed with ubiquitin-expressing plasmids and Ste6-expressing plasmids in different combinations: (1) YEp96 Ub + pRK109 = single-copy *STE6*; (2) YEp105 Ub-c-myc; (3) YEp105 Ub-c-myc + pRK69 = 2μ-*STE6*; (4) YEp105 Ub-c-myc + pRK89 = C-terminal fragment of *STE6* on 2μ vector; (5) YEp105 Ub-c-myc + pRK109 = single-copy *STE6*. Ub = ubiquitin; Ub-c-myc = ubiquitin with c-myc tag. The sizes of marker proteins in kDa are indicated.

immunoprecipitated with anti-c-myc antibodies and analysed with anti-Ste6 antibodies on Western blots. Although the signals were fainter, this experiment gave essentially the same result (not shown).

The apparent size of the protein smear in the immunoprecipitation experiment is somewhat different from that observed in the experiment described in Figure 3B. Also, there is not much difference in the appearance of the protein smear of full-size and half-size Ste6. This is probably due to protein aggregation, i.e. the appearance of the protein smear does not reflect the true size of the protein conjugates. We and others (Kuchler *et al.*, 1993) have observed that Ste6, like other multispanning membrane proteins, is prone to aggregation upon heating in SDS–sample buffer.

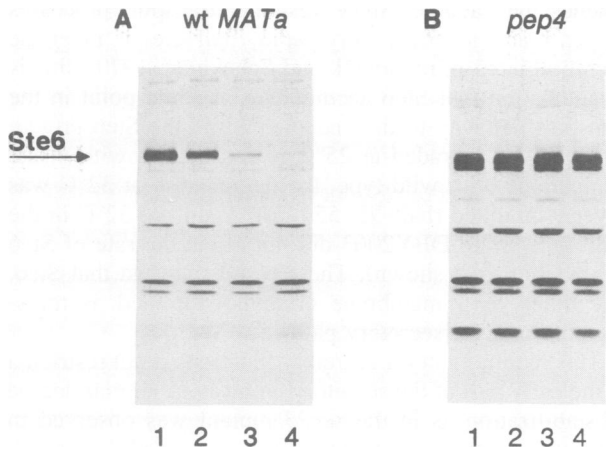

Fig. 5. Turnover of the Ste6 protein. The half-life of Ste6 was analysed by pulse–chase experiments. Cells were labelled with [^{35}S]methionine for 15 min and then chased with an excess of cold methionine, cysteine and $(NH_4)_2SO_4$. Ste6 was immunoprecipitated from cell extracts prepared at time intervals. The precipitated proteins were analysed by SDS–PAGE and autoradiography. (**A**) DBY2063 (wild-type *MAT***a** strain): lane 1, 0; lane 2, 15; lane 3, 30; and lane 4, 45 min of chase. (**B**) RKY494 (*pep4-3*): lane 1, 0; lane 2, 10; lane 3, 20; and lane 4, 30 min of chase. The position of the Ste6 band is indicated by an arrow.

Ste6 is stabilized in mutants defective in ubiquitin conjugation and in a vacuolar mutant

To find out whether the ubiquitination of Ste6 acts as a degradation signal, we examined the half-life of Ste6 in mutants defective in ubiquitin conjugation. There are now ~10 ubiquitin conjugating enzymes (E2s) known in yeast which transfer ubiquitin from the ubiquitin activating enzyme (E1) to their (largely unknown) substrates. *UBC4* and *UBC5* have been implicated in the turnover of short-lived and abnormal proteins (Seufert and Jentsch, 1990). Loss in Ubc4 and Ubc5 function also leads to a 2-fold stabilization of the only natural ubiquitinated yeast protein known so far, the transcription factor MATα2 (Chen *et al.*, 1993).

First, we determined the half-life of Ste6 in the *MAT***a** wild-type strain DBY2063 by pulse–chase experiments. The results of this and all following pulse–chase experiments are summarized in Table II. The cells were grown in sulfate-depleted minimal medium (generation time ~3 h) and then labelled for 15 min with [^{35}S]methionine. A chase was initiated by adding an excess of cold methionine and aliquots were taken after time intervals. The Ste6 protein was immunoprecipitated and analysed by SDS–PAGE and autoradiography. The Ste6 signals were quantitated by scanning of the autoradiograms. As can be seen in Figure 5A, Ste6 is an extremely unstable protein (calculated half-life 13 min). The same experiment was performed with the *ubc4* mutant YWO14 and the *ubc4 ubc5* double mutant YWO22 (Figure 6). The half-life of Ste6 in the *ubc4* mutant calculated from these experiments was comparable with wild type (14 min; Figure 6A and C). In the *ubc4 ubc5* double mutant, however, the Ste6 protein was stabilized ~3-fold (half-life 41 min; Figure 6B and C). This is in the same range as the stabilization reported for short-lived and abnormal proteins in yeast (Seufert and Jentsch, 1990) and for the MATα2 transcription factor (Chen *et al.*, 1993). The instability could be restored by transforming the *ubc4 ubc5* double mutant strain with a multicopy plasmid carrying the *UBC5* gene (half-life 13 min; not shown). Another indication that the Ste6 protein which accumulates in the plasma membrane

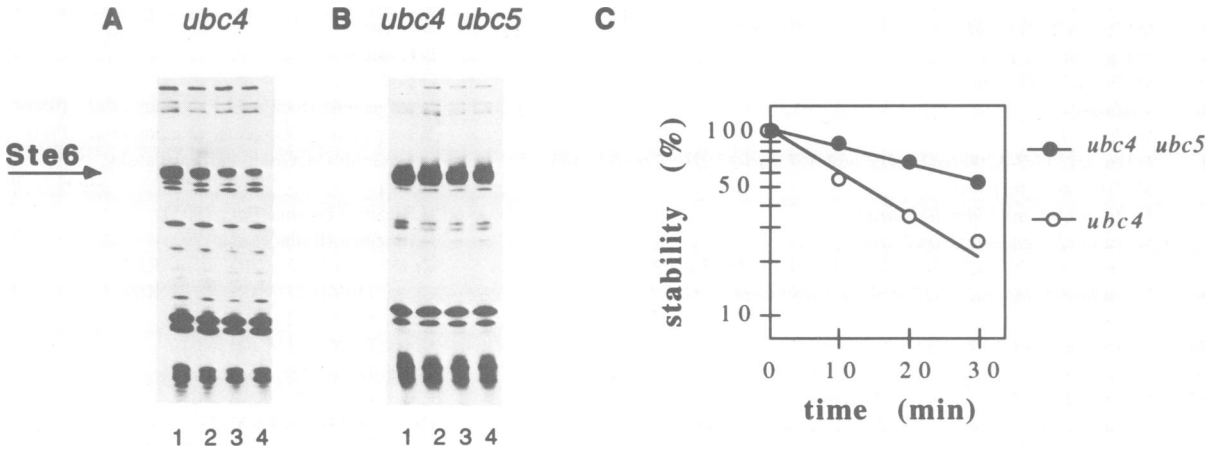

Fig. 6. Stability of Ste6 in *ubc* mutants. Cells were labelled with [^{35}S]methionine for 15 min and then chased with an excess of cold methionine, cysteine and $(NH_4)_2SO_4$. Ste6 was immunoprecipitated from cell extracts prepared at time intervals. The precipitated proteins were analysed by SDS–PAGE and autoradiography. (**A**) YWO14 (*ubc4*). (**B**) YWO22 (*ubc4 ubc5*). Lane 1, 0; lane 2, 10; lane 3, 20; and lane 4, 30 min of chase. The position of the Ste6 band is indicated by an arrow. (**C**) The Ste6 signals of the autoradiograms were quantitated by densitometry. The signal intensity (logarithmic scale) was plotted against the time of the chase.

fraction in endocytosis mutants is undergoing proteolysis is the appearance of a 57 kDa Ste6-derived protein band (Figure 3A and B). This band co-localizes with the plasma membrane ATPase marker.

Our experiments implicate the ubiquitin system in the degradation of the Ste6 protein. There is, however, abundant evidence that in mammalian cells the lysosome has an import role in the degradation of plasma membrane proteins (Hare, 1990). We therefore examined the half-life of Ste6 in a *pep4* mutant having a defect in the vacuolar protease A (Ammerer *et al.*, 1986). This protease is central to the proteolytic function of the vacuole. The Ste6 protein was dramatically stabilized in this mutant (Figure 5B) with an estimated half-life >2 h. The instability could be restored by transforming the strain with a plasmid containing the wild-type *PEP4* gene (half-life 13 min). Thus, most of the Ste6 protein seems to be degraded in the vacuole, at least in the wild-type strain. If Ste6 is degraded in the vacuole it should accumulate in this organelle when the Pep4 function is inactivated. This could indeed be shown by double-labelling immunofluorescence experiments with a *pep4* strain transformed with the plasmid carrying the epitope-tagged *STE6* gene. As can be seen from Figure 7A and B, the Ste6 staining perfectly co-localizes with the staining of the vacuolar protease CPY. The immunofluorescence staining is found at the positions of the vacuoles which can be seen as light spots in the phase-contrast image (Figure 7C).

Secretory functions are required for efficient degradation of Ste6

To see whether secretory functions are involved in the transport of Ste6 to the vacuole, we examined the degradation kinetics of Ste6 in secretory mutants (the results are summarized in Table II). The first experiment was performed with a *sec23* mutant which has a block in secretion between the ER and the Golgi complex at non-permissive temperature (Novick *et al.*, 1980, 1981). Cultures of the *sec23* mutant were incubated for 30 min at permissive (25°C) or non-permissive temperature (32°C), and then labelled for 5 min with [^{35}S]methionine. A chase was initiated with cold methionine and proteins were immunoprecipitated with anti-Ste6 antibodies from samples taken at 10 min intervals. The immunoprecipitates were analysed by SDS–PAGE and autoradiography (Figure 8). The Ste6 signals of the autoradiograms were quantitated by densitometry (Figure 9). In the cells grown at permissive temperature, the Ste6 protein was stable up to a chase period of 20 min, whereafter it was quickly degraded (half-life 11 min). The same delay in the degradation of Ste6 was observed in a wild-type strain (not shown). Therefore, it takes ~20 min before the Ste6 protein reaches the vacuole. Since vesicular transport processes in yeast are generally very rapid (half-life of invertase secretion is ~5 min; Novick and Schekman, 1979), this is an indication that Ste6 accumulates at some point in the transport pathway to the vacuole. While the Ste6 protein was quickly degraded at 25°C in *sec23* cells with a rate comparable with wild-type, the degradation at 32°C was severly inhibited (half-life 55 min). A shift to 32°C in the wild-type strain DBY2063 did not affect the rate of Ste6 degradation (not shown). These results suggest that Ste6, like other yeast membrane proteins examined, is transported along the secretory pathway.

This requirement for secretory functions is not restricted to the early part of the secretory pathway. A similar degree of stabilization as in the *sec23* mutant was observed in the late secretory mutants *sec4-1* and *sec4-2* (Novick *et al.*, 1980, 1981). These mutants are affected in the transport step between the Golgi and plasma membrane. The half-lives of Ste6 at non-permissive temperature (35°C) were 40 min (*sec4-1*) and 44 min (*sec4-2*). These

Table I. Yeast strains

Strain	Genotype	Source
DBY1389	*MATa ade2*	D.Botstein
DBY1827	*MATα his3-Δ200 leu2-3,112 ura3-52*	D.Botstein
DBY1829	*MATα ade2 his3-Δ200 leu2-3,112 lys2-801 trp1-1*	D.Botstein
DBY2062	*MATa his4-619 leu2-3,112*	D.Botstein
DBY2063	*MATa leu2-3,112 ura3-52*	D.Botstein
HMSF1	*MATa sec1-1*	Yeast genetic stock center (Novick *et al.*, 1980)
HMSF13	*MATa sec4-2*	Yeast genetic stock center (Novick *et al.*, 1980)
JPY201	*MATa gal2 his3-Δ200 leu2-3,112 lys2-801 ste6-Δ1::HIS3 trp1-1 ura3-52*	J. McGrath (McGrath and Varshavsky, 1989)
RC1713	*MATα pep4-3 trp1 ura3*	J.Ernst
RH266-1D	*MATa bar1-1 end3 his4 leu2 ura3*	H.Riezman (Raths *et al.*, 1993)
RH268-1C	*MATa bar1-1 end4 his4 leu2 ura3*	H.Riezman (Raths *et al.*, 1993)
RKY335	*MATa his3-Δ200 leu2-3,112 lys2-801 ste6-Δ1::HIS3 ura3-52*	Cross: DBY1827 × JPY201/pRK69
RKY338	*MATa his3-Δ200 leu2-3,112 ste6-Δ1::HIS3 ura3-52 GAL$^+$*	Cross: DBY1827 × JPY201/pRK69
RKY494	*MATa leu2-3,112 pep4-3 ura3*	Cross: DBY2062 × RC1713
RKY556	*MATa end4 his3-Δ200 leu2-3,112 ura3*	Cross: DBY1827 × RH268-1C
RKY560	*MATa sec4-1 ura3-52 SUC$^+$*	Cross: DBY1389 × YTX20
RKY562	*MATa end4 his3-Δ200 leu2-3,112 ste6-Δ1::HIS3 ura3-52*	Cross: RKY335 × RKY556
RKY590	*MATa his3-Δ200? sec1-1 ste6-Δ1::HIS3 ura3-52 GAL$^+$*	Cross: HMSF1 × RKY335
RKY592	*MATa end4 gal– his3-Δ200 leu2-3,112 ste6-Δ1::HIS3 ura3-52 trp1-1*	Cross: DBY1829 × RKY562/pRK109
YTX20	*MATα his4 leu2 lys2 sec4-1 ura3*	M.Egerton via T.Sommer
YTX30	*MATa his4 leu2 sec23-1 ura3*	M.Egerton via T.Sommer
YWO14	*MATa his3-Δ200 leu2-3,112 lys2-801 trp1-1 ubc4::HIS3 ura3-52*	W.Seufert (Seufert and Jentsch, 1990)
YWO22	*MATa his3-Δ200 leu2-3,112 lys2-801 trp1-1 ubc4::HIS3 ubc5::LEU2 ura3-52*	W.Seufert (Seufert and Jentsch, 1990)

Table II. Metabolic half-life of Ste6 in different strains

Strain	Genotype	Plasmid	Half-life (min)[a]
DBY2063	wild type		13
YWO14	*ubc4*		14
YWO22	*ubc4 ubc5*		41
YWO22	*ubc4 ubc5*	pSEYUBC5	18[b]
RKY494	*pep4-3*		>120
RKY494	*pep4-3*	CBZ1B1 (*PEP4*)	14[b]
RKY560/28°C	*sec4-1*		25
RKY560/35°C	*sec4-1*		40
HMSF13/28°C	*sec4-2*		19
HMSF13/35°C	*sec4-2*		44
YTX30/25°C	*sec23-1*		11
YTX30/32°C	*sec23-1*		55
RKY590/25°C	*sec1-1 Δste6*	pRK175	23
RKY590/37°C	*sec1-1 Δste6*	pRK175	61
RKY338/25°C	*Δste6*	pRK175	22[b]
RKY338/37°C	*Δste6*	pRK175	16[b]

[a]The Ste6 bands were quantitated by scanning of autoradiograms and the half-life (τ) was determined from the slope (*m*) of a semi-logarithmic plot of stability versus the chase period (τ = log 2/*m*).
[b]Single experiments, all other experiments have been performed at least twice.

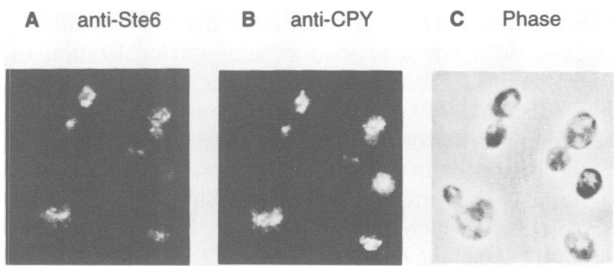

Fig. 7. Localization of Ste6 in a *pep4* mutant: double-labelling immunofluorescence experiment. Strain: RKY494 transformed with a plasmid carrying the epitope-tagged *STE6* gene. (**A**) The epitope-tagged Ste6 protein was visualized with mouse anti-c-myc primary antibodies and anti-mouse FITC-conjugated secondary antibodies. (**B**) The vacuolar protease CPY was detected with rabbit anti-CPY primary antibodies and anti-rabbit rhodamine-conjugated secondary antibodies. (**C**) Phase-contrast image.

mutants seem to have a partial defect at permissive temperature (28°C) since the Ste6 half-lives at this temperature (*sec4-1*: 25 min; *sec4-2*: 19 min) were longer than that of the wild type (13 min). This is also reflected by a slower growth rate compared with wild-type.

To make predictions about the identity of the compartment where Ste6 accumulates, we looked at the fate of the Ste6 protein pre-existing at the time of the shift to non-permissive temperature. If the Ste6 protein accumulates upstream of the secretory block, e.g. in a Golgi compartment, its further degradation should be prevented in the late secretory mutant at non-permissive temperature. If the Ste6 protein accumulates downstream of the secretory block, e.g. in a post-plasma membrane or endosomal compartment, the degradation of pre-existing Ste6 should be unaffected by the secretory block. To be able to analyse the fate of Ste6 pre-existing at the time of the shift to non-permissive temperature, Ste6 expression was placed under the control of the *GAL1* promoter (Johnston and Davis, 1984). Under these conditions, Ste6 expression is dependent on the carbon source in the growth medium. On galactose medium Ste6 is synthesized, while on glucose-containing medium Ste6 expression is repressed. We now examined the fate of Ste6 in the *sec1-1 Δste6* strain RKY590 transformed with a single-copy *GAL-STE6* plasmid. The cells were pre-grown on galactose medium at permissive temperature and then placed in glucose-containing medium pre-warmed to 25°C (permissive temperature) or 37°C (non-permissive temperature). Cell extracts were prepared at time intervals and analysed by Western blotting (Figure 10). The Ste6 signals on the nitrocellulose filters were quantitated by densitometry (Figure 11). The observed half-lives of Ste6 in the *sec1-1* strain were similar to those obtained with the other *sec* mutants (25°C = 23 min; 37°C = 61 min). The half-lives of Ste6 in a *STE6* disruption strain transformed with the *GAL1-STE6* plasmid, which is wild type with respect to the secretion phenotype, were 22 min (25°C) and 16 min (37°C). Since a block in secretion between Golgi and the plasma membrane affects the degradation of pre-existing Ste6 protein, it can be concluded that Ste6 accumulates in a compartment upstream of the *sec1-1* block, like for example in a Golgi compartment.

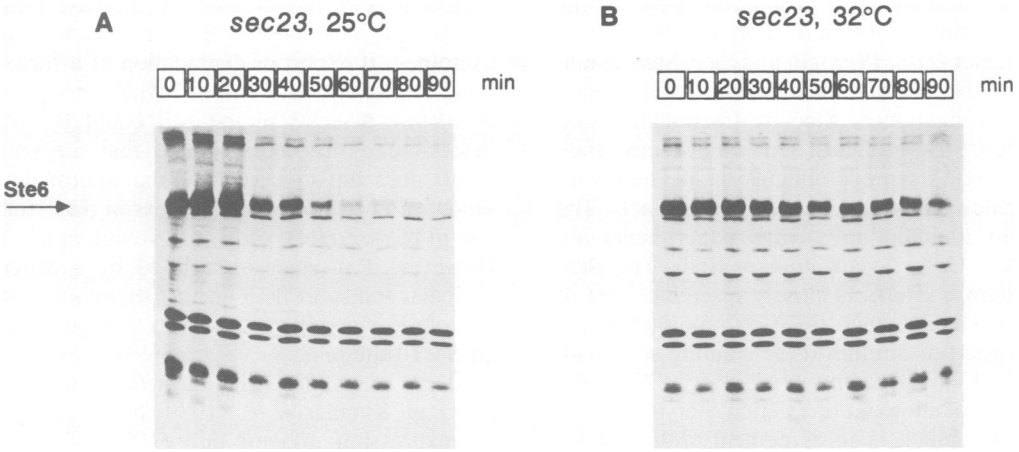

Fig. 8. Turnover of Ste6 in a *sec23* mutant. Cells of the strain YTX30 (*MATa sec23*) were incubated for 30 min at 25°C or 32°C and then labelled with [^{35}S]methionine for 5 min. After initiation of a chase by the addition of an excess of cold methionine, cysteine and $(NH_4)_2SO_4$, Ste6 was immunoprecipitated from cell extracts prepared after time intervals as indicated on top of the diagrams. The samples were analysed by SDS–PAGE and autoradiography. (**A**) 25°C; (**B**) 32°C. The position of the Ste6 protein is indicated by an arrow.

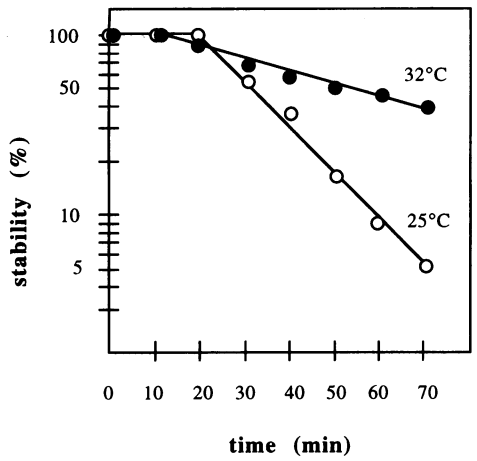

Fig. 9. Stability of Ste6 in a *sec23* mutant. The Ste6 signals of the autoradiograms shown in Figure 8 were quantitated by densitometry. The signal intensity (logarithmic scale) was plotted against the time of the chase.

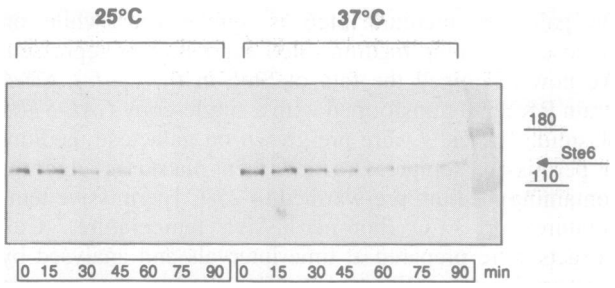

Fig. 10. Turnover of Ste6 in a *sec1-1* mutant. Cells of the *sec1-1* Δ*ste6* strain RKY590 transformed with the *GAL1-STE6* plasmid pRK175 were pre-grown at 25°C on galactose-containing medium. At time $t = 0$, the cells were transferred to glucose-containing medium and further incubated at 25°C or shifted to 37°C. Cell extracts prepared at time intervals, as indicated in the diagram, were analysed by Western blotting with anti-Ste6 antibodies. The sizes of marker proteins in kDa and the position of the Ste6 protein are given.

Discussion

It has been suggested that the ABC-transporter Ste6 secretes **a**-factor by forming a channel or pore in the plasma membrane through which **a**-facter is released into the medium (Kuchler *et al.*, 1993). In this case, Ste6 should be detectable in the plasma membrane. We examined the subcellular localization of Ste6 by fractionation and immunofluorescence experiments. Our data demonstrate that the Ste6 protein is predominantly associated with internal membranes and not with the cell surface. The fractionation and immunofluorescence experiments are compatible with a Golgi localization of Ste6. The Ste6 profile on the sucrose gradients closely resembles that of the Golgi protein DPAP A and the Ste6 immunofluorescence staining pattern is similar to the staining seen with the Golgi protein Kex2 (Redding *et al.*, 1991). Also, the finding that the degradation of pre-existing Ste6 is affected by a late secretory block is in agreement with a Golgi localization of Ste6.

Despite its mainly intracellular localization, Ste6 also seems to have access to the plasma membrane, as demonstrated by the accumulation of Ste6 in the plasma membrane in endocytosis mutants. It is not clear whether this reflects the wild-type situation or whether this accumulation in the plasma membrane is the consequence of the endocytosis defect. In clathrin mutants, which are partially defective in the endocytosis of α-factor, mislocalization of the Golgi proteins Kex2 and DPAP A to the cell surface has been observed (Seeger and Payne, 1992). The endocytosis defect caused by the *end3* and *end4* mutations, however, does not lead to a general mislocalization of Golgi proteins to the plasma membrane, as we could not detect Kex2 and DPAP A in the plasma membrane fraction. Therefore, it is reasonable to assume that a certain fraction of Ste6 is present in the plasma membrane under normal conditions. This minor fraction of Ste6 could be the active species which secretes **a**-factor, but an intriguing possibility is that the internal fraction of Ste6 is functioning in **a**-factor secretion, e.g. by sequestering **a**-factor into vesicles which are delivered to the plasma membrane. A similar mechanism of secretion has been proposed for interleukin (IL)-1α and IL-1β, which like **a**-factor are secreted by a non-classical pathway (Rubartelli *et al.*, 1990).

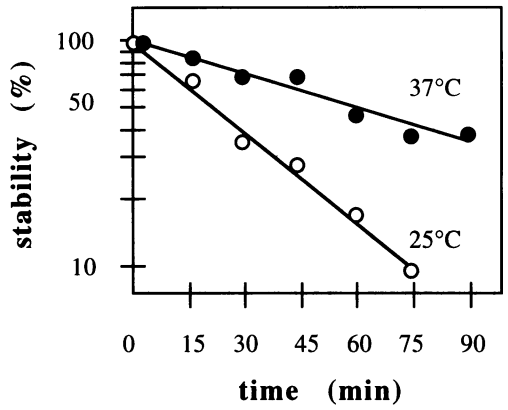

Fig. 11. Turnover of Ste6 in a *sec1-1* mutant. The Ste6 signals of the Western blot shown in Figure 10 were quantitated by densitometry. The signal intensity (logarithmic scale) was plotted against the time of the chase.

It has been claimed that pro-**a**-factor, the **a**-factor precursor, is not sequestered into vesicles as it is not protected from degradation by protease (Kuchler *et al.*, 1989), but the fate of mature **a**-factor has not been examined. If export or degradation of **a**-factor is fast, this issue is probably difficult to address because the amount of mature **a**-factor in the cell could be too low to be detectable. It has been argued that the secretion of **a**-factor does not involve vesicular intermediates since its secretion is not blocked by a loss in Sec1 function acting late in the secretory pathway (Novick *et al.*, 1980, 1981). However, if **a**-factor is secreted by a different type of vesicular transport than normal secretory proteins, e.g. as part of the endocytic pathway, its transport may not depend on Sec1 function.

There is evidence that **a**-factor enters the endocytic pathway. Kuchler *et al.* (1989) have shown that in cells overexpressing **a**-factor only 3–5% of the radioactivity incorporated into the pro-**a**-factor precursor is secreted into the medium. Theoretically, if all precursor was processed, 50% of the incorporated label would have been expected to appear in the medium in the form of mature

a-factor. Furthermore, they found that a significant larger fraction of mature **a**-factor could be secreted in a *pep4* mutant strain, indicating that a large fraction of **a**-factor is degraded in the vacuole. Thus, either **a**-factor enters the vacuole directly by translocation across the vacuolar membrane or it is transported to the vacuole within a vesicular carrier. In both cases, it is reasonable to assume that Ste6 is responsible for transporting **a**-factor across the membrane.

The Ste6 protein has a very short half-life. What is the reason for this instability? One possible explanation is that in natural homothallic yeast strains, which undergo mating-type switching, the Ste6 protein is only required for a short period of time. Therefore, a long half-life would not be desirable.

The Ste6 protein is mainly degraded in the vacuole, as demonstrated by the striking stabilization observed in the vacuolar *pep4* mutant. Secretory functions are required for efficient degradation of Ste6, i.e. for its transport to the vacuole, indicating that Ste6 enters the secretory pathway. However, in all secretory mutants examined the degradation of Ste6 was not completely prevented by imposing a secretory block. This suggests that an alternative pathway exists for the degradation of Ste6 which does not depend on the secretory functions tested. Since the stabilization of Ste6 is much more pronounced in the *pep4* mutant than in the secretory mutants, this pathway probably also involves the vacuole. A candidate for such a pathway could be an autophagic process (Takshige *et al.*, 1992) which could well be induced by stress conditions like a block in secretion.

The existence of more than one pathway for the degradation of Ste6 is also suggested by the finding that Ste6 is ubiquitinated. One function of the covalent attachment of ubiquitin to proteins is to mark them for degradation by an ATP-dependent protease complex (Finley and Chau, 1991; Hershko and Ciechanover, 1992; Jentsch, 1992). The existence of proteins which are ubiquitinated, but metabolically stable, suggests that the ubiquitination can serve other functions besides acting as a degradation signal. Stable proteins are usually mono-ubiquitinated, while proteolytic substrates are mostly modified by the attachment of a branched multi-ubiquitin chain. From the appearance on gels, Ste6 seems to be multiply ubiquitinated. Further support for an involvement of the ubiquitin system in the degradation of Ste6 comes from the finding that Ste6 is stabilized ~3-fold in a mutant where the two ubiquitin conjugating enzymes Ubc4 and Ubc5 are inactivated (Seufert and Jentsch, 1990). The pronounced stabilization of Ste6 in the *pep4* mutant, however, suggests that Ste6 is primarily degraded in the vacuole. So, what is the relationship between these two different degradative pathways? One possibility is that Ste6 is degraded by two independent pathways, a vacuolar and a cytosolic ubiquitin-dependent pathway. According to this view, the degradation in the vacuole would be the major route of degradation of Ste6. The Ubc4- and Ubc5-dependent pathway could be especially important in a situation where the vacuolar pathway is overloaded or blocked, like in the endocytosis mutants. In line with this interpretation is that Ubc4 and Ubc5 are mainly stress-inducible proteins. Alternatively, ubiquitination could be required to direct the Ste6 protein into the vacuolar degradation pathway, e.g. by acting as an endocytosis signal or by altering the structure of Ste6 in such a way that an endocytosis signal is exposed. Since a loss in Ubc4 and Ubc5 function does not completely eliminate the degradation of Ste6, one would have to assume that Ste6 can be recognized by other ubiquitin-conjugating enzymes. This has indeed been shown for the MATα2 transcription factor, where in addition to Ubc4 and Ubc5 two other Ubc proteins are involved in its degradation (Chen *et al.*, 1993). There are also reports that protein–ubiquitin conjugates are enriched in lysosomes, supporting the view that ubiquitination can act as a signal for lysosomal or vacuolar degradation (Laszlo *et al.*, 1990). Another possibility is that a vacuolar and a cytosolic proteolytic system are required for complete degradation of Ste6 because it is difficult to rationalize how the large portions of Ste6 which, according to the topological model of Ste6 (Kuchler *et al.*, 1989; McGrath and Varshavsky, 1989), are located at the cytoplasmic face of the membrane can be degraded by vacuolar enzymes.

Despite a detailed knowledge about the enzymes involved in the ubiquitination of proteins, only few specific substrates are known. Ste6 is now the second yeast protein, in addition to MATα2, that has been shown to be ubiquitinated. The identification of Ste6 as a specific substrate for the ubiquitin system offers the opportunity to investigate how specific proteins are selected for ubiquitination and what the signals are that are recognized by ubiquitinating enzymes.

Materials and methods

Media and strains

The yeast strains were grown in rich medium (YPD) containing 1% Bacto Yeast extract (Difco), 2% Bacto Peptone (Difco) and 2% glucose, or in minimal medium (SD) containing 0.7% yeast nitrogen base without amino acids (Difco), 1% casamino acids (Difco) and 2% glucose supplemented with uracil and tryptophan as required. For the pulse–chase experiments cells were grown in MV medium (Rothblatt and Schekman, 1989). For yeast strains see Table I.

Preparation of affinity-purified anti-Ste6 antibodies

The preparation of trpE–Ste6 fusion protein from strain HB101 containing the plasmid pRK53 was carried out essentially as described for the trpE–Mlp1 protein (Kölling *et al.*, 1993).

Plasmid constructions

The plasmid pRK69 carries a 6.2 kb *Bgl*II–*Sal*I *STE6* fragment cloned into the 2μ vector YEp420 (Ma *et al.*, 1987). On plasmid pRK89, which is derived from YEp420, the C-terminal half of Ste6, starting at position 1824 of the *STE6* sequence (Kuchler *et al.*, 1989), is expressed under the control of the *PDC1* promoter (Kellermann and Hollenberg, 1988). The plasmid pRK109 contains the 6.2 kb *Bgl*II–*Sal*I *STE6* fragment on the centromere plasmid YCp50 (Rose *et al.*, 1987). The plasmid pRK175, based on the vector pBM272 (Johnston and Davis, 1984), contains the *STE6* gene on a 5.4 kb *Bsp*HI–*Sal*I fragment under the control of the *GAL1* promoter. A *trpE–STE6* fusion was constructed (pRK53) by inserting the 1.2 kb *Nco*I–*Eco*RI fragment from the C-terminal part of *STE6* into the *Sma*I site of pATH10 (Dieckmann and Tzagoloff, 1985). Blunt ends were generated by fill-in with Klenow polymerase. The plasmids YEp96 and YEp105 are described in Hochstrasser *et al.* (1991) and the *STE6-c-myc* plasmid is described in Kuchler *et al.* (1993). The plasmid pSEYUBC5, obtained from Stefan Jentsch, is a 2μ vector which contains the *UBC5* gene. The plasmid CBZ1B1 carrying the *PEP4* gene is described in Woolford *et al.* (1986).

Fractionation experiments

Exponentially growing cells (OD_{600} = 0.5–1.0, 3–6 × 10^7 cells/ml) from a 100 ml culture were harvested, washed once in cold 10 mM

NaN_3 and once in STED10 [10% (w/w) sucrose, 10 mM Tris–Cl (pH 7.6), 10 mM EDTA, 1 mM dithiothreitol (DTT)]. After resuspending the cells in 0.5 ml STED10 (+ protease inhibitors: 0.5 μg/ml each of aprotinin, antipain, chymostatin, leupeptin, pepstatin A, and 1.6 μg/ml benzamidine, 1 μg/ml phenanthroline and 170 μg/ml phenylmethylsulfonylfluoride), glass beads were added up to the top of the liquid and the suspension was vortexed for 2 min. After the addition of another 1 ml of STED10, the extract was transferred to a fresh tube and spun at 500 *g* for 5 min to remove cell debris. About 1 ml of the cleared cell extract was loaded onto a sucrose gradient prepared the following way. In a SW40 centrifuge tube 4 ml of STED50 (53% sucrose), STED35 (35% sucrose) and STED20 (20% sucrose) were layered on top of each other [STED = sucrose, 10 mM Tris–Cl (pH 7.6), 1 mM EDTA, 1 mM DTT]. The centrifuge tubes were slowly turned into a horizontal position. After 3–5 h of horizontal diffusion, the gradients were again turned into an upright position, loaded with extract and spun for 13–17 h at 30 000 r.p.m. in a SW40 rotor at 4°C; 700 μl fractions were collected from the top of the gradient.

Enzyme assays

NADPH cytochrome c oxidoreductase. The redox change in the absorbance spectrum of cytochrome *c* upon reduction by the enzyme is measured. The reaction mixture consists of KP_i (100 mM, pH 7.0), 1 mM KCN, NADPH (100 μM) and cytochrome *c* (25 μM) in its oxidized form; 20–50 μl of the gradient fractions are added and the initial rate of increase in absorbance at 550 nm is registered in a spectrophotometer. α-*Mannosidase*. The assay measures the generation of the yellow *p*-nitrophenol from the non-coloured glycoside. To 250 μl of the reaction mixture (50 mM KP_i, 0.04% Triton X-100, 1 mM *p*-nitrophenyl-α-mannoside) are added 50 μl of the gradient fractions. After incubating the samples at 30°C for 2 h, 600 μl of 2% Na_2CO_3 are added to stop the reaction. The absorbance at 400 nm is then determined.

Immunofluorescence microscopy

Cells were grown overnight in SD medium + 1% casamino acids to a density of 1–2 × 10^7 cells/ml. The cells were then further incubated for 1 h at 25°C or at 36°C. They were then fixed for 2 h with formaldehyde which was directly added to the culture medium (5% final concentration). Sphaeroplasting and antibody staining were performed as described in Pringle *et al.* (1989) with the modification that the fixed sphaeroplasts were permeabilized by incubation in sphaeroplasting buffer containing 0.1% Triton X-100 for 5 min at room temperature. Cells were photographed with Kodak Tri-X 400 black and white film on a Zeiss standard microscope equipped for epifluorescence.

Immunoprecipitation and pulse–chase experiments

The experiments were basically performed as described previously (Franzusoff *et al.*, 1991). The yeast cells were grown overnight in minimal medium (MV) in which all sulfate salts are replaced by chloride salts supplemented with 100 μM $(NH_4)_2SO_4$ (Rothblatt and Schekman, 1989). The generation time in this medium was ~3 h at 25°C for a wild-type strain. Typically 5 OD_{600} units (3 × 10^8 cells) of exponentially growing cells were harvested and resuspended in fresh MV medium to a density of 2 OD_{600}. The cells were labelled by adding 25 μCi of [^{35}S]methionine/OD_{600} of cells. The labelling period was between 5 and 30 min. For pulse–chase experiments, a concentrated chase solution (100 mM $(NH_4)_2SO_4$, 0.3% cysteine, 0.4% methionine) was diluted 100-fold into the culture. Aliquots of ~1 OD_{600} unit of cells were removed at time intervals, washed in cold 10 mM NaN_3 and resuspended in 100 μl lysis buffer [0.3 M sorbitol, 10 mM MOPS (pH 7.5), 0.1% NaN_3] + protease inhibitors. Lysis was achieved by vortexing the suspension with glass beads for 2 min. After the addition of 1 vol of 2× sample buffer [4% SDS, 125 mM Tris–Cl (pH 6.8), 20% glycerol, 20 mM DTT, 0.02% bromophenol blue], the lysate was incubated at 50°C for 30 min or at 37°C for 1 h. The Ste6 protein and PMATPase did not enter the gel when the samples had been solubilized by boiling in sample buffer. The best results for the PMATPase were obtained with a solubilization temperature of 37°C. Then 4 vols of IP dilution buffer [1.25% Triton X-100, 190 mM NaCl, 6 mM EDTA, 60 mM Tris–Cl (pH 7.6)] were added and the insoluble material was removed by centrifugation. Following an overnight incubation at 4°C with 1–5 μl of antiserum, 50 μl of a 20% suspension of protein A–Sepharose beads (Pharmacia) were added and the samples were incubated for another 3 h at room temperature. The beads were washed three times with IP buffer [1% Triton X-100, 0.2% SDS, 150 mM NaCl, 5 mM EDTA, 50 mM Tris–Cl (pH 7.6)] diluted 1:2 with 2× sample buffer and incubated for 30 min at 50°C. About half of the immunoprecipitated material was loaded onto an SDS gel. The gels were fixed in a mixture of acetic acid (7%) and methanol (20%), soaked in Amplify (Amersham) to enhance the signal, dried and exposed to Kodak X-Omat AR film for ~3 days.

Acknowledgements

We thank Rainer Roggenkamp for his help in preparing the Ste6 antibodies, and Dieter Gallwitz, Ramon Serrano and Tom Stevens for sending us antibodies. We also thank Jürgen Dohmen, Stefan Jentsch, Beth Jones, Karl Kuchler, John McGrath, Howard Riezman, Wolfgang Seufert and Thomas Sommer for sending us strains or plasmids. Furthermore, we would like to thank Karl Kuchler for helpful discussions and comments on the manuscript. This work was supported by the BMFT project 'Stoffumwandlung mit Biokatalysatoren'.

References

Ammerer,G., Hunter,C.P., Rothman,J.H., Saari,G.C., Valls,L.A. and Stevens,T.H. (1986) *Mol. Cell. Biol.*, **6**, 2490–2499.
Cenciarelli,C., Hou,D., Hsu,K.-C., Rellahan,B.L., Wiest,D.L., Smith,H.T., Fried,V.A. and Weissman,A.M. (1992) *Science*, **257**, 795–797.
Chen,P., Johnson,P., Sommer,T., Jentsch,S. and Hochstrasser,M. (1993) *Cell*, **74**, 357–369.
Davis,N.G., Horecka,J.L. and Sprague,G.F. (1993) *J. Cell Biol.*, **122**, 53–65.
Denning,G.M., Anderson,M.P., Amara,J.F., Marshall,J., Smith,A.E. and Welsh,M.J. (1992) *Nature*, **358**, 761–764.
Dieckmann,C.L. and Tzagoloff,A. (1985) *J. Biol. Chem.*, **260**, 1513–1520.
Finley,D. and Chau,V. (1991) *Annu. Rev. Cell Biol.*, **7**, 25–69.
Franzusoff,A., Rothblatt,J. and Schekman,R. (1991) *Methods Enzymol.*, **194**, 662–674.
Glotzer,M., Murray,A.W. and Kirschner,M.W. (1991) *Nature*, **349**, 132–138.
Hare,J.F. (1990) *Biochim. Biophys. Acta*, **1031**, 71–90.
Hershko,A. and Ciechanover,A. (1992) *Annu. Rev. Biochem.*, **61**, 761–807.
Higgins,C.F. (1992) *Annu. Rev. Cell Biol.*, **8**, 67–113.
Hochstrasser,M., Ellison,M.J., Chau,V. and Varshavsky,A. (1991) *Proc. Natl Acad. Sci. USA*, **88**, 4606–4610.
Jabben,M., Shanklin,J. and Vierstra,R.D. (1989) *J. Biol. Chem.*, **264**, 4998–5005.
Jentsch,S. (1992) *Annu. Rev. Genet.*, **26**, 179–207.
Johnston,M. and Davis,R.W. (1984) *Mol. Cell. Biol.*, **4**, 1440–1448.
Kellermann,E. and Hollenberg,C.P. (1988) *Curr. Genet.*, **14**, 337–344.
Kölling,R., Nguyen,T., Chen,E.Y. and Botstein,D. (1993) *Mol. Gen. Genet.*, **237**, 359–369.
Kuchler,K., Sterne,R.E. and Thorner,J. (1989) *EMBO J.*, **8**, 3973–3984.
Kuchler,K., Dohlman,H.G. and Thorner,J. (1993) *J. Cell Biol.*, **120**, 1203–1215.
Laszlo,L., Doherty,F.J., Osborn,N.U. and Mayer,R.J. (1990) *FEBS Lett.*, **261**, 365–368.
Leung,D.W., Spencer,S.A., Cachianes,G., Hammonds,R.G., Collins,C., Henzel,W.J., Barnard,R., Waters,M.J. and Wood,W.I. (1987) *Nature*, **330**, 537–543.
Ma,H., Kunes,S., Schatz,P.J. and Botstein,D. (1987) *Gene*, **58**, 201–216.
McGrath,J.P. and Varshavsky,A. (1989) *Nature*, **340**, 400–404.
Novick,P. and Schekman,R. (1979) *Proc. Natl Acad. Sci. USA*, **76**, 1858–1862.
Novick,P., Field,C. and Schekman,R. (1980) *Cell*, **21**, 205–215.
Novick,P., Ferro,S. and Schekman,R. (1981) *Cell*, **25**, 461–469.
Paolini,R. and Kinet,J.-P. (1993) *EMBO J.*, **12**, 779–786.
Pringle,J.R., Preston,R.A., Adams,A.E., Stearns,T., Drubin,D.G., Haarer,B.K. and Jones,E.W. (1989) *Methods Cell Biol.*, **31**, 357–434.
Raths,S., Rohrer,J., Crausaz,F. and Riezman,H. (1993) *J. Cell Biol.*, **120**, 55–65.
Raymond,M., Gros,P., Whiteway,M. and Thomas,D.Y. (1992) *Science*, **256**, 232–233.
Redding,K., Holcomb,C. and Fuller,R.S. (1991) *J. Cell Biol.*, **113**, 527–538.
Riezman,H. (1993) *Trends Cell Biol.*, **3**, 273–277.
Roberts,C.J., Nothwehr,S.F. and Stevens,T.H. (1992) *J. Cell Biol.*, **119**, 69–83.

Rose,M.D., Novick,P., Thomas,J.H., Botstein,D. and Fink,G.R. (1987) *Gene*, **60**, 237–243.
Rothblatt,J. and Schekman,R. (1989) *Methods Cell Biol.*, **32**, 3–36.
Rubartelli,A., Cozzolino,F., Talio,M. and Sitia,R. (1990) *EMBO J.*, **9**, 1503–1510.
Seeger,M. and Payne,G.S. (1992) *J. Cell Biol.*, **118**, 531–540.
Seufert,W. and Jentsch,S. (1990) *EMBO J.*, **9**, 543–550.
Siegelman,M., Bond,M.W., Gallatin,W.M., St John,T., Smith,H.T., Fried,V.A. and Weissman,I.L. (1986) *Science*, **231**, 823–829.
Singer,B. and Riezman,H. (1990) *J. Cell Biol.*, **110**, 1911–1922.
Smith,R.M., Charron,M.J., Shah,N., Lodish,H.F. and Jarett,L. (1991) *Proc. Natl Acad. Sci. USA*, **88**, 6893–6897.
Takshige,K., Baba,M., Tsuboi,S., Noda,T. and Ohsumi,Y. (1992) *J. Cell Biol.*, **119**, 301–311.
Vida,T.A., Huyer,G. and Emr,S.D. (1993) *J. Cell Biol.*, **121**, 1245–1256.
Woolford,C.A., Daniels,L.B., Park,F.J., Jones,E.W., Van Arsdell,J.N. and Innis,M.A. (1986) *Mol. Cell. Biol.*, **6**, 2500–2510.
Yarden,Y. *et al.* (1986) *Nature*, **323**, 226–232.

Received on February 16, 1994; revised on April 28, 1994